

simply on a comparison of areas, and is given in Fig. 2.

It remains to prove that the electric field distribution is indeed convex. For the set of Eqs. (A1), (A2), (A3a), and (A3b) in their full generality and with the boundary conditions: $\mathcal{E}=0$ at $x=0$ and at $x=L$, we can only conjecture at this point that the \mathcal{E} curve has the postulated convexity. For the class of cases studied analytically in Appendix A it can be verified algebraically that the field is convex, and $\mathcal{E}_M/(V/L)$ can be directly computed and shown to be less than two. However, for investigation of the more general cases a combination of geometrical and analytical methods¹¹ will likely prove more fruitful.

We illustrate here the application of this technique to the case of the perfect insulator, $n_T=p_T=z_R=0$. Substituting for p - n from Eq. (A2) in Eq. (A4), $(d/dx)[\mathcal{E}(d\mathcal{E}/dx)] = -e(b+1)r/\epsilon\mu_n$ and is therefore everywhere negative. Assuming a single maximum in \mathcal{E} , say at x_M , then the plot of \mathcal{E} vs x must be convex. If it were not, say it was as plotted in Fig. 3, then the plot of $d\mathcal{E}/dx$ would have to be as shown. Taking two positions, say x_1 , and $x_2 > x_1$, such that $(d\mathcal{E}/dx)_1 = (d\mathcal{E}/dx)_2$, it follows from Fig. 3 that $[\mathcal{E}(d\mathcal{E}/dx)]_2 > [\mathcal{E}(d\mathcal{E}/dx)]_1$, whence $d/dx[\mathcal{E}(d\mathcal{E}/dx)]$ must be posi-

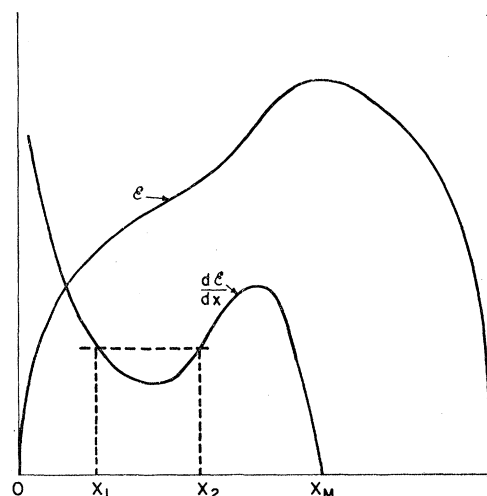


FIG. 3. Proof, by contradiction (see text), that the electric-field distribution must be convex for double injection into a perfect insulator.

tive somewhere between x_1 and x_2 , and we have reached a contradiction. In like manner it is shown that \mathcal{E} can have only a single maximum between $x=0$ and $x=L$.

Current-Voltage Characteristics of Forward Biased Long p - i - n Structures

R. D. LARRABEE

RCA Laboratories, Princeton, New Jersey

(Received August 12, 1960)

The current-voltage characteristics have been observed in several germanium p - i - n structures in which the n side was biased negative and the p side positive so as to cause a double injection of electrons and holes into the structure. The middle i section was constructed of good quality germanium (approximately 2×10^{13} donors/cm³) and was many minority carrier diffusion lengths long. The observed I - V characteristics display a low-field region in which the current is proportional to the voltage followed by a higher field region in which the current is proportional to the square of the voltage. In the square-law region, the current is a function of the difference, rather than the sum, of the thermal densities of the electrons and holes. These observations lend experimental support to the basic theories of Lampert and Rose regarding volume-controlled double injection into a semiconductor.

THE preceding paper¹ outlined a theory regarding the current-voltage characteristics of long semiconductor specimens provided with one contact which injected electrons and another which injected holes. This paper will describe some relatively simple experiments in which the measured current-voltage characteristics of suitable specimens lend support to these theoretical considerations.

Germanium was selected as the most suitable material for study since its technology is so far advanced compared to the other semiconductors. Since it was desired to measure the sample characteristics in the

presence of double injection in which the density of injected carriers was large compared to the extrinsic density, it was necessary to utilize the highest resistivity material available. A germanium crystal with an extrinsic density of about 2×10^{13} electrons/cm³ and a low level bulk lifetime of approximately 600 μ sec was selected. It should be noted, however, owing to the perturbing influence of the surfaces of the specimens utilized and the high injection levels employed, it is not certain that this low-level bulk lifetime should be used in the quantitative comparison of theory and experiment.

Since the theoretical considerations were concerned with the case in which the diffusion length could be

¹ M. Lampert and A. Rose, preceding paper [Phys. Rev. **121**, 26 (1961)].

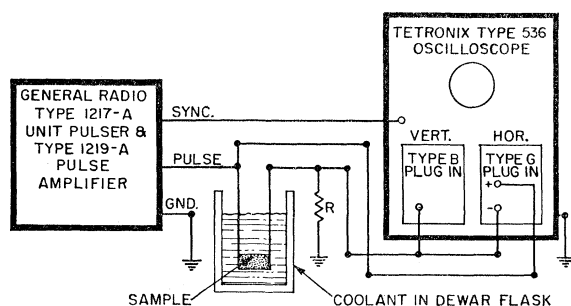


FIG. 1. Schematic diagram of the basic circuit utilized in the measurement of the current-voltage characteristics (the type 545 oscilloscope used to view the current and/or voltage as a function of time is not shown in this diagram).

neglected in comparison with the sample length, it was necessary to use relatively long specimens (approximately one cm). The cross-sectional area of the specimen was limited by the lowest resistance which could be measured by the equipment utilized for the measurement of the current-voltage curves. In the present experiments, a rectangular cross section of approximately one mm square was selected. With this small cross-sectional dimension, the minority carrier lifetime was essentially determined by the nature of the exposed surface areas of the specimen (in all the experiments

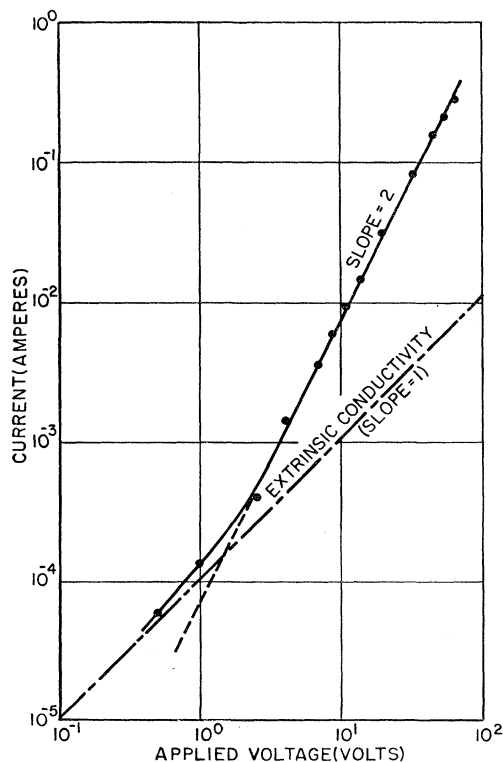


FIG. 2. The current-voltage characteristics of a high-purity *n*-type specimen, 0.97 cm long, 0.097 cm by 0.097 cm square cross section, temperature = 0°C. The extrinsic density = 2×10^{18} electrons/cm³.

mentioned in this paper the specimen was equipped with a strong accumulation surface). The electron-injecting contact consisted of an alloy of tin and 4% antimony and the hole-injecting contact was an alloy of indium and $\frac{1}{2}$ % gallium. These contacts were alloyed on the ends of the specimen in a hydrogen atmosphere at 550°C.

It was necessary to use pulse techniques in measuring the current-voltage characteristics to avoid heating the specimen at the higher voltages. A pulse length of 600 μ sec and a repetition rate of one pulse per second were sufficiently long to allow steady-state conditions to be reached but not long enough to heat the specimen

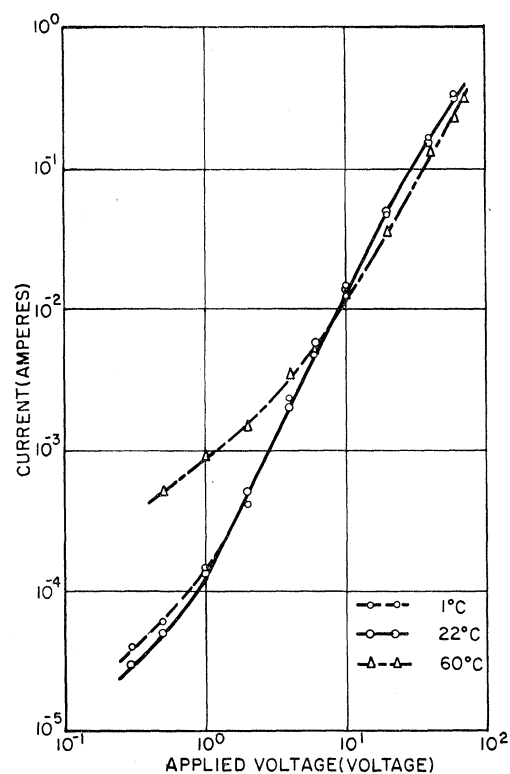


FIG. 3. The current-voltage characteristics of a high-purity *n*-type specimen at various temperatures. The specimen was 0.97 cm long, 0.063 cm by 0.055 cm in cross section, and the data were taken at the indicated temperatures.

appreciably. The pulser consisted of a General Radio Type 1217-A unit pulser and a Type 1219-A pulse amplifier. The sample voltage and current were observed both on a Tetronix type 536 oscilloscope (current as a function of voltage) and on a Tetronix type 545 oscilloscope (current and voltage as a function of time). The current and voltage were recorded near the termination of the pulse (steady-state conditions). Figure 1 illustrates the basic circuit utilized in this measurement.

Figure 2 is a typical current-voltage characteristic (see figure caption for experimental details). Notice

that over most of the range the current is proportional to the square of the voltage as predicted by the previous theoretical considerations.¹ The tendency of the curve to approach a linear form equal to the conductivity of the extrinsic majority carriers is evident at low voltages.

Figure 3 illustrates the effect of thermal pair density by comparing data similar to Fig. 2 at different temperatures. Notice that at the lower temperatures (where the material can be considered an extrinsic semiconductor) the current-voltage characteristics are very similar (compare data at 1°C with data at 22°C). The slight difference between these two curves is probably due to the variation of mobility with temperature. However, at the highest temperature, the number of electrons and holes generated thermally across the band gap is so much greater than the extrinsic carrier density (the material is now approximately an intrinsic semiconductor) that the low field region is dominated by their presence. However, at the higher fields, the curve approaches the same quadratic curve that was obtained at lower temperatures (except for the temperature dependence of the mobility). This indicates that the mechanisms operative in the quadratic region of the curve do not depend upon the sum of the thermal pair density but rather suggest that they depend on the difference in the thermal pair density (or the uncom-

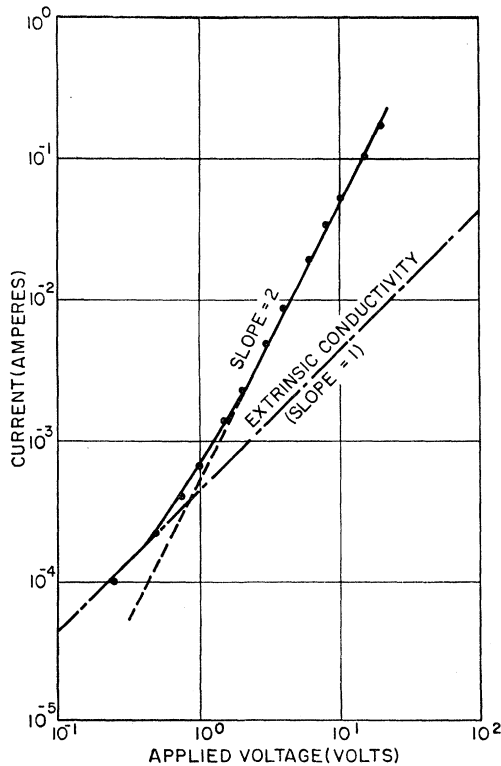


FIG. 4. The current-voltage characteristics of a high-purity *p*-type specimen, 0.91 cm long, 0.117 cm by 0.096 cm cross section, temperature = 0°C. The extrinsic density = 1.3×10^{14} holes/cm³.

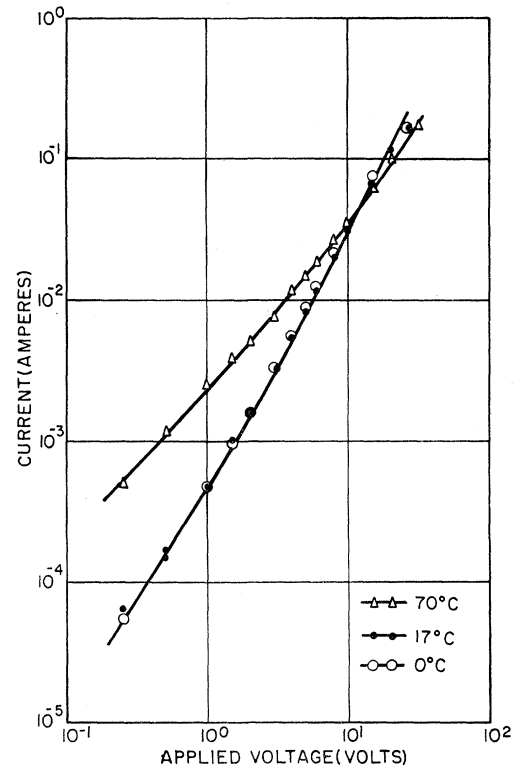


FIG. 5. The current-voltage characteristics of a high-purity *p*-type specimen at various temperatures. The specimen was 0.91 cm long, 0.117 cm by 0.096 cm cross section, and the data were taken at the indicated temperatures.

pensated impurity density) which remains constant with temperature.

It was desired for the sake of completeness, to attempt the same experiment with specimens constructed from high-purity *p*-type material instead of the high-purity *n*-type material utilized in the previous experiments. Figures 4 and 5 represent a summary of the data so obtained. Comparison of Figs. 2 and 4 and Figs. 3 and 5 will reveal that the same basic results quoted above for the experiments with *n*-type material are evident in the *I-V* data with *p*-type material.

Consequently, it has been demonstrated that the current-voltage characteristics of suitably chosen germanium samples display three properties that were theoretically predicted by Lampert and Rose¹: first, a linear region at low applied voltages; second, a quadratic region at higher voltages; and third, a dependence in the quadratic region on the difference in the thermal pair density rather than upon the sum. It is therefore felt that these experiments lend support to these theoretical ideas. However, due to the complexities introduced by the lifetime being dominated by the surface and the lack of a complete quantitative experimental comparison, it is felt that the present experiments do not directly confirm, but rather lend support, to some of the major implications of the Lampert-Rose theory.